Refining Light-Based Positioning for Indoor Smart Spaces

E.W. Lam
Boston University
Boston, MA
emilylam@bu.edu

T.D.C. Little
Boston University
Boston, MA
tdcl@bu.edu

ABSTRACT

Visible light positioning, or VLP, has emerged as a low-cost approach to enabling a variety of indoor location-based services for indoor smart spaces. However, a survey of existing approaches to VLP reveals some challenges in comparing one system to another.

Advances in key areas are expected to enable new levels of performance at low cost. These include innovations at the source (LEDs, Laser Diodes/LIDAR, and ToF sensors), at the receiver (diversity receivers and AoA sensors), and in the design of the overall end-to-end VLP system. Again, comparing these improvements from one system to the another is difficult due to varying assumptions and operating conditions.

In this paper we classify VLP techniques in an attempt to reconcile the wide range of characteristics. We also propose a new concept called an *active zone* in recognition that best performance is needed primarily in a subset of the volume of an indoor space. Finally, we show the performance of a baseline VLP system under the new metric and conclude with how our Visible Light Communication (VLC) testbed can be used to verify and quantify the region we call the *active zone*.

CCS CONCEPTS

• **Networks** → *Location based services*; Network mobility; • **Hardware** → *Emerging optical and photonic technologies*;

KEYWORDS

Visible light positioning, localization, location based services, optical wireless communications, visible light communications, LiFi, smart spaces, testbeds, active zone.

ACM Reference Format:
E.W. Lam and T.D.C. Little. 2018. Refining Light-Based Positioning for Indoor Smart Spaces. In *SMARTOBJECTS'18: 4th ACM MobiHoc Workshop on Experiences with the Design and Implementation of Smart Objects, June 25, 2018, Los Angeles, CA, USA.* ACM, New York, NY, USA, 8 pages. https://doi.org/10.1145/3213299.3213308

1 INTRODUCTION

The economic benefits of GPS (or more broadly GNSS) are substantial, with billons of satellite based devices in use worldwide. But GPS is an outdoor technology unable to reliably penetrate into buildings. Positioning for applications in indoor smart spaces lags in adoption due to the lack of low-cost, readily deployable positioning technology that can achieve repeatable sub-centimeter accuracy.

Candidate technologies for indoor positioning include the use of RF (e.g. WiFi or Bluetooth), UWB, ultrasound, image analysis, and lighting. Our work on indoor positioning is in the lighting domain, typically as a function piggybacked on the lighting mission using overhead luminaries, known as "Visible Light Positioning" (VLP). In this domain, a variety of recent component technologies have emerged and are being explored to realize new performance levels. These technologies include innovations at the sources (LEDs, Laser Diodes/LIDAR, ToF sensors), at the receivers (diversity receivers and AoA), and in the design of the overall end-to-end VLP system [3, 8, 10, 12, 15].

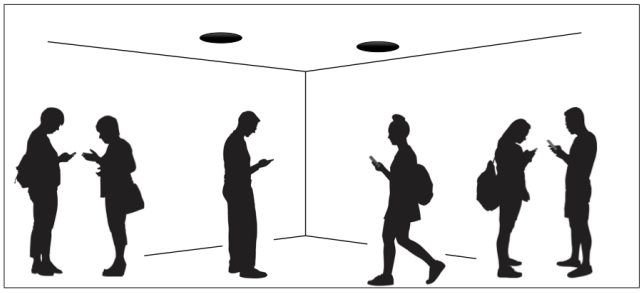

Figure 1: Indoor Positioning – Locating People, Objects, and Devices

Indoor positioning, sometimes called "indoor GPS," continues to be an attractive new technology that is expected to have great commercial impact with new benefits in terms of human convenience, productivity, and efficiency. We also consider positioning – or localization – to be an essential function enabling any "smart" application. Contemporary examples of indoor position and related location based services (LBS) include, along with their primary benefits:

- Tracking physicians in hospitals (productivity)
- Navigating to departure gates in an airport (productivity)
- Automatic light and temperature control in the home (convenience, efficiency)
- Serving coupons to a mobile device in a mall based on location (efficiency)
- Delivering audio to visitors in a museum as a virtual tour guide (convenience)
- Steering robots in a "pick and pack" facility (productivity)

These are just a few important applications, but there are many more. The basic scenario for indoor positioning is illustrated in

SMARTOBJECTS'18, June 25, 2018, Los Angeles, CA, USA

ACM ISBN 978-1-4503-5857-6/18/06…$15.00
https://doi.org/10.1145/3213299.3213308

Fig. 1. Here we focus on positioning of people, and are able to use, but are not required to, the availability of a mobile device on each person.

Across four years of competition, the real-world accuracy of RF solutions is at best in the decimeter range [7]. In juxtaposition, light-based positioning shows promise of centimeter accuracy. In this work we focus on light-based indoor positioning technologies and our experiences therein. In contrast to RF, particularly WiFi based solutions, light is usually more proximal to targets of interest and is not attenuated unpredictably by walls. Light is deployed in occupied spaces near where it is needed and thus has inherent signal qualities. Light-based indoor positioning is also a piggyback technology that does not require separate installation.

We introduce a new concept of an *active zone* within an indoor volume. The concept emerges from our efforts to establish relevant positioning metrics based on our observations in a Visible Light Communication (VLC) testbed. We have found existing metrics to be flawed in that they consider spaces to be homogeneous when in fact they are not; nor are they used in a homogeneous way. The *active zone* concept allows us to consider the positioning performance within a region of interest that dominates the activity within the space.

The remainder of the paper is organized as follows. In Section 2 we classify the dimensions of indoor positing techniques including their attributes and mathematical basis. We also highlight VLP and describe the complications in benchmarking competitive work. Section 3 focuses on the proposed *active zone* and a baseline model for studying VLP. Section 4 describes what can be expected in translating simulated work into a real smart space. Section 5 concludes the paper.

2 CHARACTERIZING LIGHT-BASED POSITIONING

2.1 General Classifications

In an effort to benchmark different VLP technologies, we have realized that there is a wide variety of design choices that impact not only performance but are themselves important for realizing specific goals such as low cost, privacy preservation, and complexity of components. These design choices are not only valid for VLP but rather for the general realm of indoor positioning. Here we sort out the characteristics of the range of solutions. The main distinctions are:

- **Active vs. Passive:** A passive system attempts to position people or objects without any help from attached electronics. Carrying an active badge or bluetooth fob would be considered an active approach. Using cameras to locate people would be passive.
- **Privacy-preserving or not:** A privacy preserving approach would rely on a device (e.g., a smartphone) to establish its position based on observed signals. GPS works this way. A system in which a mobile device is located by infrastructure is not (e.g., access point ranging). In addition, receiver types play a factor in privacy preservation. Camera based approaches will capture entire frames of activities while a single photodiode (PD) will not capture individual attributions.
- **Piggybacked or Standalone:** Using ambient signals such as preexisting lighting or WiFi constitutes piggybacked methods. Installing bluetooth beacons or cameras represent a standalone system.
- **Mapped or Unmapped:** A mapped system can provide cues and reference data to support positioning whereas an unmapped space must be discovered, dictating a different strategy for positioning. Mapped spaces require investment in up front surveys and subsequent maintenance. Fingerprinting walks a fine line between a mapped and unmapped system as it relies heavily on the environment.
- **Monostatic or Bistatic:** A monostatic system is one in which a transmitting fixture, such as a luminaire, and a receiver, such a PD, are co-located. In contrast, a bistatic system is comprised of transmitter(s) and receiver(s) separated by space. LIDAR is a monostatic system (single device) whereas GPS is bistatic (satellites and GPS device). Systems that require precise timing synchronization fair better on monostatic systems where the transmitter and receiver are co-located.
- **Physical Modalities:** Physical modalities concern the means or the types of raw information collected. These includes: angle of arrival (AOA) of a signal, received signal strength (RSS), and time of arrival (TOA) of a signal. These can also include images in imaging based techniques and mapping information collected in a LIDAR system.
- **Mathematical Techniques:** Mathematical techniques range from geometric based algorithms, e.g., trilateration and triangulation, to machine learning techniques, such as fingerprinting to a feature database, to image processing. The mathematical technique selected will rely on the physical modalities selected and the device processing capability.

2.2 Visible Light Positioning Performance

VLP typically is an infrastructure-less, bistatic, and active indoor positioning system capable of all the physical modalities and mathematical techniques described above. These distinctions contribute to another important classification for VLP: performance metrics.

The primary metric for VLP performance is accuracy required for positioning, that is highly dependent on the use case. For example, in the virtual tour guide example, an audio narration should be triggered when a device is within viewing range of an exhibit; probably on the order of 1-2m. But in, for example, a retail setting such as a supermarket, a 1m accuracy may not be sufficient to identify which product a customer is considering. Likewise, fine positioning, for example locating fingers for a virtual keyboard will need a higher resolution still.

While accuracy is important, benchmarking accuracy between systems is difficult. Errors are often calculated for a given plane of operation (typically a fixed height), which does not consider the inhomogeneous nature of a 3D volume. When 3D errors are considered, this is often extended to be errors over a fraction (2D plane) of the target volume, or as a CDF of the accuracy of the target volume.

In Table 1, we summarize and classify the state of the art using standard metrics. However, we have substantial difficulty in

Table 1: Survey of Recent VLP: Characteristics and Performance

Technology	Infrastructure	Dimensions	Physical	Mathematical	Accuracy (plane or volume)
[11]	No, Bistatic, Rx	2D	RSS	Fingerprinting	14cm (1.2m × 1.8m @ 1m)
[14]	No, Bistatic, RX	2D	RSS ranging	Trilateration	5.9cm (6m × 6m × @ 3m)
[1]	No, Bistatic, RX	2D	RSS ranging	Trilateration	2.4cm ($0.6m^3$ triangle @ 0.6m)
[10]	No, Bistatic, RXs	3D	RX-AOA	Triangulation	10cm (5m × 5m @ 2m)
[12]	No, Bistatic, tilted RXs	3D	RX-AOA, RSS	Triangulation	6cm (2m × 2m × 2.5m)
[3]	No, Bistatic, RX, Laser	3D	RX-AOA, RSS	Triangulation	12.89cm (6m × 6m @ 3m)
[8]	No, Bistatic, Synced TXs, RX	3D	TOA	Trilateration	0.1cm (5m × 5m × 3m)
[13]	No, Bistatic, Camera	3D	RSS	Imaging	6cm (1.2m × 1.2m @ 1.2m)
[5]	Yes, Bistatic, RXs	Sensing	RSS	Light Blockage	Gestures (3.6m × 4.8m)
[15]	Yes, Monostatic, RXs	2D	RSS	Light Transport	0.6cm (2.1m × 3.6m × 2.2m)
[7]	No, Monostatic, RXs	3D	LIDAR	Proprietary	3.3cm (All)

reconciling metrics based on different operating conditions and assumptions. Particularly, space dimensions vary tremendously from work to work. In the future we would hope that researchers reference a similar configuration and test harness to evaluate performance. Similarly, some works lack specificity on metrics such as computational time, cost, or complexity.

On top of the issues discussed above, the 2D and 3D performance comparison is confusing when some techniques assume a known height. Indeed, when height is known, the accuracy of position estimation can be very high [3]. Thus fixing height is not a realistic assumption; it was a good initial approach in earlier work but is no longer sound for future work.

Based on our desire to better understand the relative performance and to focus on the parts of an indoor space that are relevant, we address the ambiguities in 3D position error. Specifically, we (a) developed a baseline VLP simulation environment and (b) propose a space utilization model called an *active zone*. These are described in the next section.

3 PROPOSED ACTIVE ZONE MODEL

Most metrics for indoor positioning treat the indoor space as homogeneous, revealing an error bound based on a fraction of the covered space. However, often only a limited volume of the space is used in any practical way. For example, mobile phones are typically operated between waist level and shoulder level, a narrow band of heights. Similarly, physical constraints such as tables, walls, and other furniture constrain the use of mobile devices to a subset of a room's volume. Lastly, certain areas have low probability of use, such as corners and areas near the ceiling. Conveniently, these locations often are poorly covered by some positioning techniques such as VLP. A meaningful metric is therefore the performance of indoor positioning within this constrained volume. As a first approximation, we define the *active zone* as the region existing between 0.75m from the floor to 2m above the floor. But really any volume where activity is concentrated and positioning error must be bounded can be defined as an *active zone*. An example of an *active zone* is shown in Fig. 2.

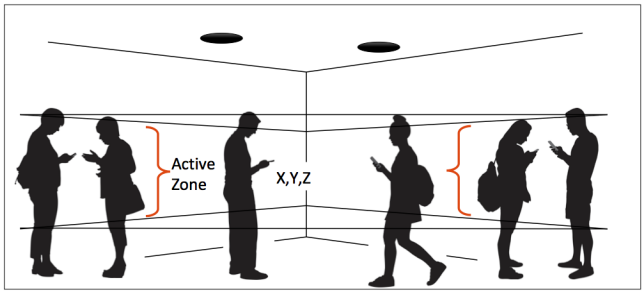

Figure 2: Active Zone from 0.75m to 2m from the Floor

Of course, this region neglects spaces that can be occupied by some smart devices (and floor-based devices – robotic vacuums) or fixed smart devices such as lighting. However, the *active zone* metric can be extended based on the use case contemplated. For example, if the scenario is to track indoor UAVs, then clearly the *active zone* must be defined to include the volume between the ceiling and any humans present.

In the following, we work up a baseline VLP model to establish a working scenario on which to demonstrate how the *active zone* concept influences claimed performance metrics in a typical use case.

3.1 Development of a Baseline VLP Model for Evaluating VLP Systems

As discussed in the previous section, there are many varieties of VLP found in the literature. Here, we elaborate a popular RSS ranging technique with straightforward implementation – ideal to implement on low power and low complexity smart objects. This bistatic, RSS-based VLP strategy relies on isolating modulated signals from fixed position light sources at the receiver for trilateration, Fig. 3. In

addition, this setup is prime for multi-target positioning and data communications using VLC.

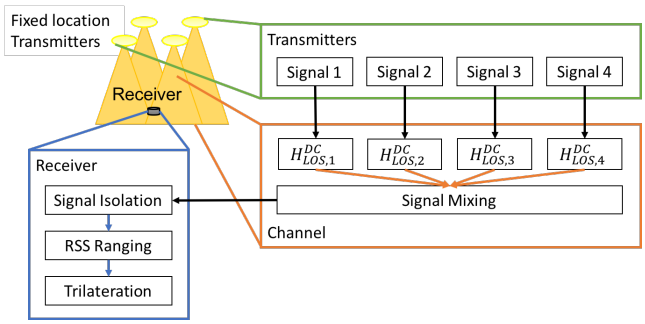

Figure 3: Bistatic RSS-based VLP Model

3.1.1 Channel Model. The most common visible light source today is the LED, as it is low cost, relatively fast, and provides good, wide field-of-view (FOV) illumination. The active receiver is fundamental a photosensitive element, which usually is a low-cost single-pixel photodiode. Line-of-sight (LOS) channel attenuations from each of these LEDs are modeled as Lambertian and is dependent on transmitter and receiver characteristics and the distance and angle between them, Fig. 4 [2, 14]:

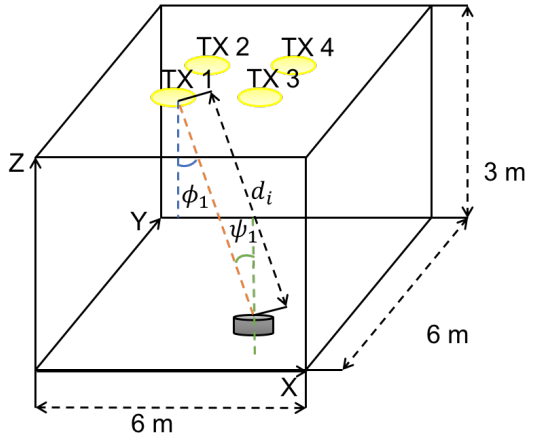

Figure 4: Lambertian Model for VLP Showing Transmitter and Receiver Geometry

$$H^{DC}_{LOS,i} = \begin{cases} R_0(\phi_i)\frac{A}{d_i^2}R_{eff}(\psi_i) * cos(\psi_i), & 0 \le \psi_i \le \Psi_c \\ 0, & \psi_i > \Psi_c \end{cases}, \quad (1)$$

where Ψ_c is the receiver concentrator FOV, A is the receiver detector area, m is Lambertian order, and for each transmitter i, ψ_i is the angle of incidence w.r.t. to receiver axis, ϕ_i is angle of radiance, and d_i is distance between transmitter i and the receiver.

$R_0(\phi_i)$ is the Lambertian radiant intensity defined as:

$$R_0(\phi_i) = \frac{m+1}{2\pi}cos^m(\phi_i), \quad (2)$$

$R_{eff}(\psi_i)$ is the effective responsivity of the photodiode, defined as the product of $T_s(\psi_i)$, the signal transmission of the filter (losses over wavelengths), and $g(\psi_i)$, the receiver concentrator gain, which relies on the refractive index, n, of the concentrator:

$$g(\psi_i) = \begin{cases} \frac{n^2}{sin^2\Psi_c} & 0 \le \psi_i \le \Psi_c \\ 0 & \psi_i > \Psi_c \end{cases}. \quad (3)$$

Furthermore, noise is modeled as white Gaussian noise (AWGN) and as such we get a final RSS at each position of the room for each transmitter as:

$$P_{r,i} = P_{t,i}H^{DC}_{LOS,i} + w, \quad (4)$$

where $P_{t,i}$ is transmitter power, $H^{DC}_{LOS,i}$ is the Lambertian channel model from above, and w is AWGN.

3.1.2 Position Estimation. Because VLP relies on gathering information from multiple light sources, it is important to be able to decouple the contributions of each light source from the raw received mixed light. The easiest way to do this is through time-domain multiplexing (TDM), which is the paradigm in which each light source transmits one at a time. This requires the transmitters to be perfectly synchronized with each other, which is possible but not ideal for dynamic room configurations [9]. There is also latency in letting the light sources transmit one at a time.

In contrast, if resources and bandwidth (BW) are not limited, frequency-domain multiplexing (FDM), in which each light transmits on its own designated frequency, is a more independent and scalable solution. There is no need for time synchronization and signals can be transmitted at the same time as the final mixed signal can be decoupled at the receiver with a fast Fourier transform (FFT) of a captured frame and RSS values can be identified at each assigned frequency. FDM is also well suited for cooperation with VLC.

In addition, locations and powers of the transmitters are usually assumed known. This is achieve either through an initial calibration step where environmental information is transferred from the infrastructure to the receiver by some form of data communications, which can be VLC or environmental information is stored locally at the receiver.

Finally, the tracked device can perform a trilateration algorithm using the RSS values from each of the transmitting luminaires and the known positions of the luminaires. This process is described in the appendix for reference.

3.2 Signal Analysis in the Baseline VLP Model

We performed two sets of simulations to understand the effects of signal coverage on VLP. The first considers planes of reference in the test space (positions) with simulated combined noise-less received signal strength values from four luminaires. The second, Section 3.3, focuses on the accuracy of an example trilateration approach when AWGN is applied. The parameters used in simulation are indicated in Table 2.

Referring to Figs. 5-8, although LEDs provide good general coverage, there remain zones in the space that suffer from poor coverage. Fig. 5 and 6 illustrate variations in RSS at different locations in the room. Fig. 5 shows a 2D horizontal RSS plane at the floor. Fig. 6

Table 2: Parameters Used in Modeling and Simulation

Parameter	Value
Room [LxWxH]	[6m x 6m x 3m]
4 Transmitters	(2, 2, 0), (2, 4, 0), (4, 2, 0), (4, 4, 0)
PD Area	1cm^2
TX Power, P_t	2W
FOV, Ψ_c	70°
Optical Filter Gain, $T_s(\psi)$	1
Refractive Index, n_c	1.5
AWGN	-25dBm

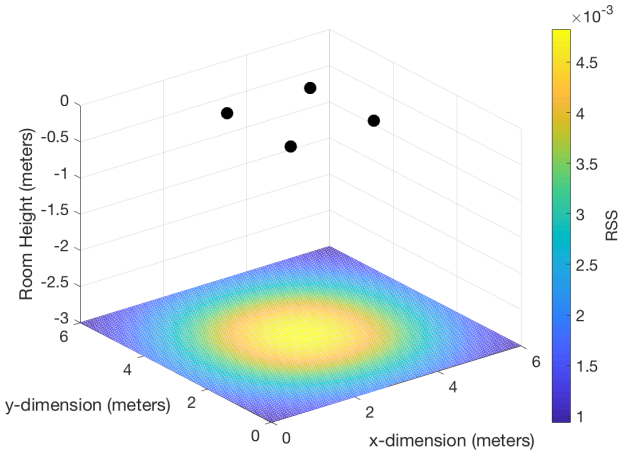

Figure 5: Baseline x-y Coverage Plane at the Floor (3m Away from Transmitters)

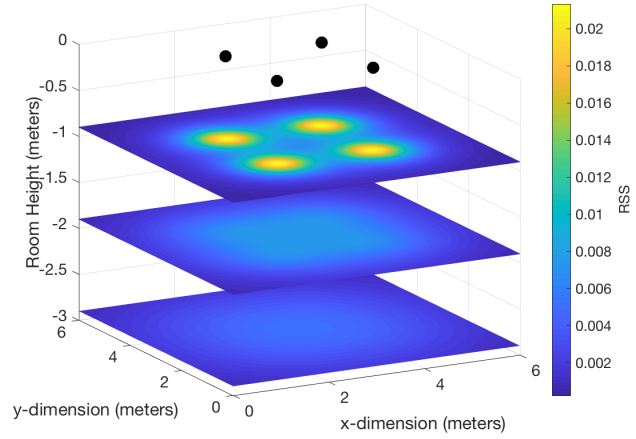

Figure 6: Baseline x-y Coverage Planes at Different Heights

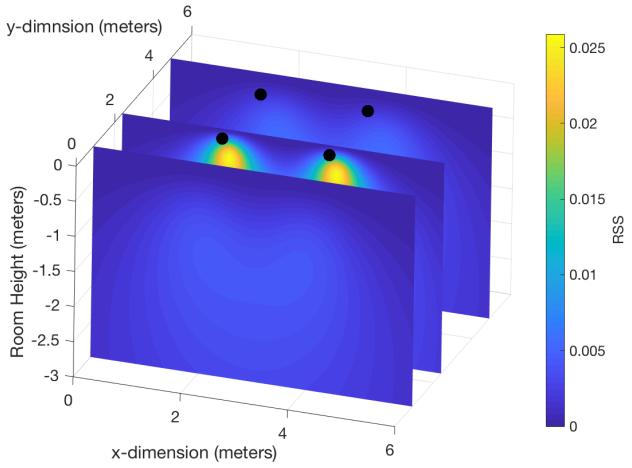

Figure 7: Baseline x-z Coverage Planes at y-dimension Depths

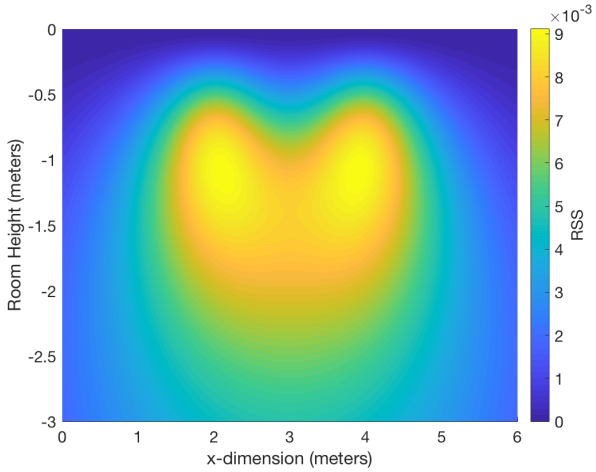

Figure 8: Baseline x-z Coverage Plane at the Center (y fixed at 3m)

shows different 2D horizontal planes at different distances from the floor including at the floor. Due to the scaling of the color-bar, the colors of the two floor planes appear different. However, the trend is noticeable: the corners exhibit poor coverage, especially closer to the ceiling. The implication is that the accuracy for trilateration near the edges and the corner is worst. This is because for a fixed noise level at the receiver, SNR is worst at the edges and corners.

Fig. 7 shows vertical planar cuts at different depths of the y-dimension of the room. The next figure, Fig. 8 shows the center cut isolated for a clearer view of the combined pattern of four luminaires in the vertical dimension. Interesting to note is that due to the radiance angle of the luminaires, combined signal is weak near the luminaires. These figures again illustrate the different SNRs possible across the planes and together with the 2D x-y planes give a

good representation of the 3D volume that will impact the accuracy of trilateration throughout the space.

As seen from the figures, there are locations with poor LOS coverage. These spaces occur at the corners and close to the ceiling. Thus, an *active zone* or good coverage region should be described when benchmarking positioning as this *active zone* is the area of interest and the other positions are negligible zones with the given assumption that nothing of importance happens in corners and near the ceiling.

3.3 RSS Trilateration in the Baseline Model

In the previous subsection, we simulated the combined RSS values from the four luminaires. Here we consider a receiver located at different planes, particularly at 3m away (the floor), 2m away (typical user height), and 1m away (upper bound on the active area). For each plane we calculate x,y estimates and the mean square error (MSE) for each receiver position (in increments of 0.05m in each dimension). We also introduce noise into the measurements, as would be expected in any real implementation. The noise is AWGN with a power of -25dbm. Fig. 9 shows the results for the 3m plane (floor level). The graphic reiterates the difficulties with position accuracy at the fringes of the space. Corners and edges have the poorest accuracy but this is also the least active area of a room, which supports our proposal to define a subset of the volume as an *active zone*.

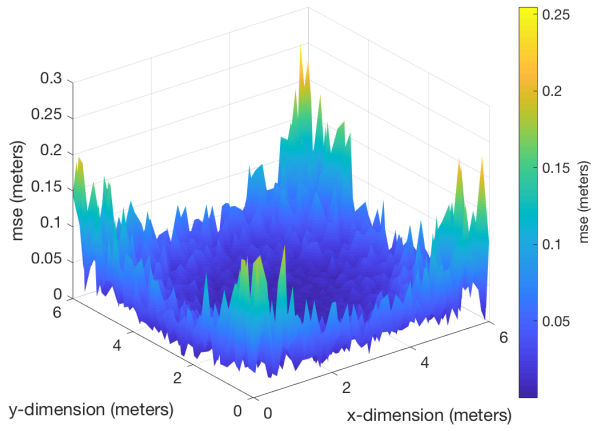

Figure 9: Spatial Map showing Estimate Errors at the Floor (3m Away from the Ceiling) for Trilateration

From the simulated MSE data, we can show a cumulative distribution function (CDF) for any plane in the space. CDF curves for the three distinct mentioned planes are plotted in Fig. 10. The results indicate a substantial difference in position estimates based on the height of the receiver. This data indicates that the best performance exists away from the luminaires (as expected), and above the floor. Being too close to the ceiling limits a receiver's FOV to multiple luminaires and will prevent trilateration from converging.

Applying constraints of 0.75m height to the 2m height and not including the corners (1m × 1m right triangle area with a height

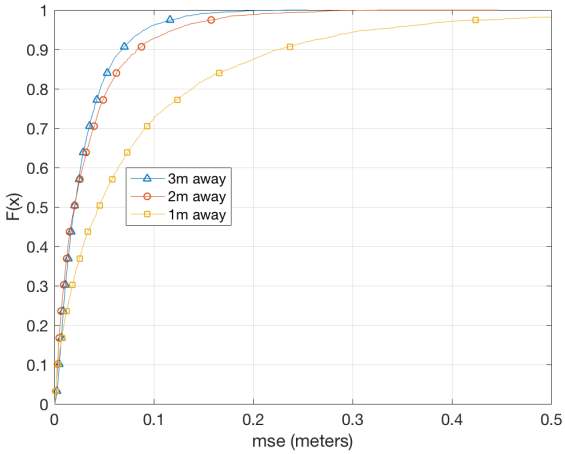

Figure 10: CDF of Estimate Errors Based on Model Simulation at Different Planes

of the entire room), we define this space as the *active zone*. Fig. 11 extends the MSE CDF analysis to what we propose as the *active zone*. Fig. 11 shows the CDF for the entire room compared to an *active zone* plus the corners, and an *active zone*. By focusing on the *active zone*, where most receivers will be active, we believe this is a better evaluation metric for VLP.

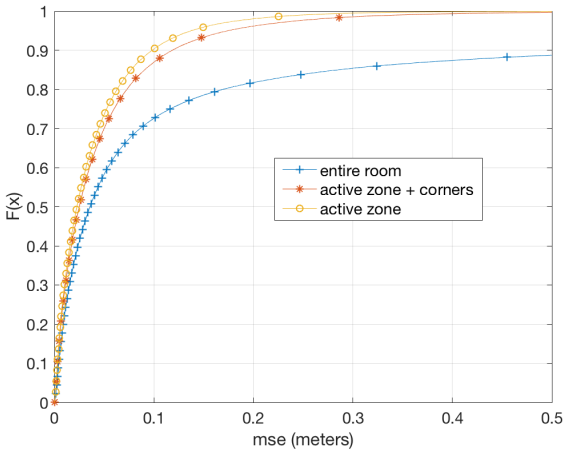

Figure 11: CDF of Estimate Errors Based on Model Simulation for Different Zones Highlighting the Contrast Between an Entire Space and Active Zone

4 TRANSLATION TO A PRACTICAL SMART SPACE

We recognize that there can be a substantial difference between simulated indoor positioning systems and practical implementations. Fortunately, we have developed an extensive testbed for studying

the performance of indoor VLC units configured as an lighting array (Fig. 12). This testbed is configured as an array of 15 luminaires driven by a Software Defined Radio (SDR) system based on a Universal Software Radio Peripheral (USRP) handware and GNURadio. A more detailed description can be found in reference [6].

In this prior work we established that the simulation model does indeed conform to the testbed in terms of predicted and measured RSS values. This outcome allows us to use the simulation as a tool to predict the behavior of similar modeled systems.

Even though we have confidence in the models, we still expect to validate our analysis of an *active zone* and in particular the performance under real system noise as is found in the testbed. The testbed also moves from the baseline model of 4 luminaires to 15, greatly increasing the diversity of RSS sources to consider.

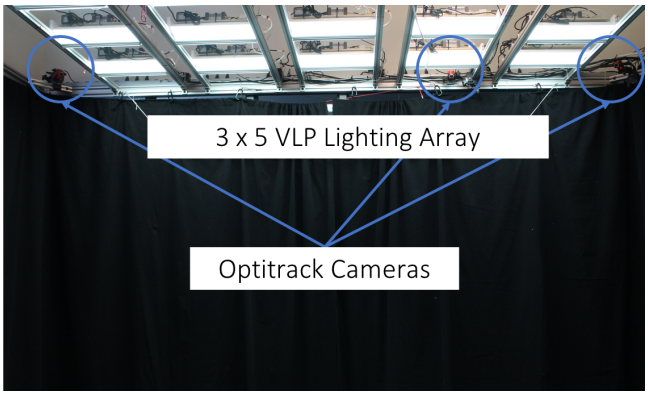

Figure 12: Multi-Cell Lighting Array Testbed

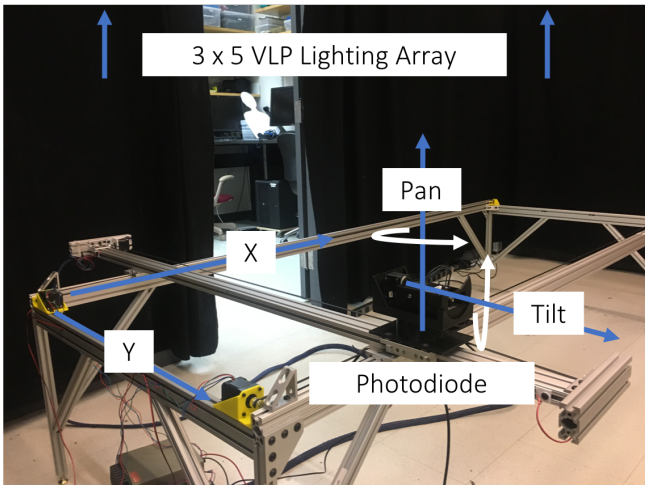

Figure 13: MATT – Mobile Activity Tracking Tool

To measure across the *active zone*, we require measuring signal strength at each X,Y point on each Z-plane through the volume. To this end we have modified our autonomous robotic measurement system (called MATT – Mobile Activity Tracking Tool) to collect a

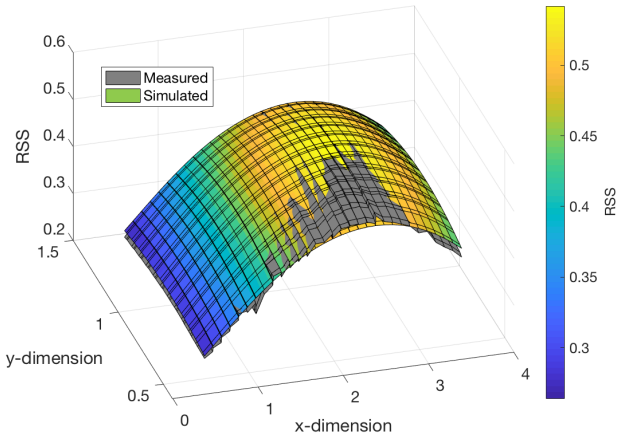

Figure 14: Comparison of MATT Measured Coverage vs. Simulated Coverage

complete data set at each plane before we change the Z increment. Salient features of MATT are: the computer control of X,Y position increments; computer control of rotation and receiver angle; and variable field of view (FOV), Fig. 13. We plan to add a mechanical crank to be able to raise the platform to different heights. Coupled with the SDR system we are able to generate unique frequency division modulation to allow a receiver to isolate the signal of any luminaire in the receiver FOV.

Fig. 14 shows one set of collected data using MATT comparing simulated coverage and measured coverage for a fixed perpendicular receiver angle and fixed height. Noticeable again is the poor coverage, combined RSS of all luminaires, along the edges of the room. This is due to the fact that RSS falls off from the center, directly under the luminaire. The lower RSS values lead to higher position estimate errors.

In addition, we use an Optitrack motion capture system to track and record receiver position and orientation, which serves as a ground truth on 3D position. Initial data reported in [6] demonstrates experimentation with measured VLP performance, however, we only report on the impact of the *active zone* on data from simulations at this time.

5 CONCLUSION

While indoor positioning has come a long way from coarse beaconing, the lack of an easy to use and ubiquitous solution remains an oppotunity for future innovation. The next generation of VLP is likely to be the result of the fusion of several modularities. Thus, it is important to be able to quantify performance of VLP systems from solution to solution. We propose a region called an *active zone* that excludes areas of low use as a metric to evaluate VLP schemes. By using this new metric we can exactly match the performance of the technique with the characteristics of the space and use case that requires indoor positioning.

APPENDIX

RSS Ranging and Trilateration

RSS ranging is calculated by solving for d_i in Eq. 1:

$$d_i = \sqrt{\frac{(m+1)Acos^m(\phi_i)R_{eff}(\psi_i)cos(\psi_i)P_{t,i}}{2\pi P_{r,i}}} \tag{5}$$

Position is estimated using a linear least square estimator to solve the trilateration equations:

$$\begin{aligned}(x_e - x_1)^2 + (y_e - y_1)^2 + (z_e - z_1)^2 &= d_1^2,\\ (x_e - x_2)^2 + (y_e - y_2)^2 + (z_e - z_2)^2 &= d_2^2,\\ (x_e - x_3)^2 + (y_e - y_3)^2 + (z_e - z_3)^2 &= d_3^2,\end{aligned} \tag{6}$$

where x_i and y_i are the x and y location of the i-th transmitter and x_e and y_e are likewise estimated x and y position respectively.

Due to a lack of height diversity among the transmitter, i.e., transmitters are all placed on the same plane, vertical distance away from the transmitting plane is fixed in simple VLP trilateration systems so that the trilateration equations can be easily solvable and d_i can be solved algebraically. Thus

$$cos(\phi_i) = H/d_i, \tag{7}$$

where H is the vertical distance away from the transmitting plane. In addition, the receiving plane and the transmitting plane are assumed parallel, $\psi = \phi$, Fig. 4, so that

$$cos(\phi_i) = cos(\psi_i). \tag{8}$$

Solving for d_i assuming Lambertian order, $m = 1$, the receiver is within transmitter FOV, $0 \le \psi_i \le \Psi_c$, and substituting Eq. 7 and 8 into Eq. 5 gives distance, range, in respect of RSS, $P_{r,i}$:

$$d_i = \sqrt{\sqrt{\frac{AR_{eff}(\psi_i)P_{t,i}H^2}{\pi P_{r,i}}} - H^2} \tag{9}$$

For 2D positioning with known height, Eq. 6 can be rewritten in the matrix-vector form of $\mathbf{AX} = \mathbf{B}$:

$$\mathbf{A} = \begin{bmatrix} x_2 - x_1 & y_2 - y_1 \\ x_3 - x_1 & y_3 - y_1 \end{bmatrix}, \tag{10}$$

$$\mathbf{B} = \begin{bmatrix} (d_1^2 - d_2^2 + x_2^2 + y_2^2 - x_1^2 - y_1^2)/2 \\ (d_1^2 - d_3^2 + x_3^2 + y_3^2 - x_1^2 - y_1^2)/2 \end{bmatrix}, \tag{11}$$

$$\mathbf{X} = \begin{bmatrix} x_e \\ y_e \end{bmatrix}, \tag{12}$$

$\mathbf{X}$ can then be solved using:

$$\mathbf{X} = (\mathbf{A}^T\mathbf{A})^{-1}\mathbf{A}^T\mathbf{B}. \tag{13}$$

ACKNOWLEDGMENTS

This work was supported in part by the Engineering Research Centers Program of the National Science Foundation under NSF Cooperative Agreement No. EEC-0812056 and by NSF No. CNS-1617924.

REFERENCES

[1] H. S. Kim, D. R. Kim, S. H. Yang, Y. H. Son, and S. K. Han. 2013. An Indoor Visible Light Communication Positioning System Using a RF Carrier Allocation Technique. *Journal of Lightwave Technology* 31, 1 (Jan 2013), 134–144. https://doi.org/10.1109/JLT.2012.2225826

[2] T. Komine and M. Nakagawa. 2004. Fundamental analysis for visible-light communication system using LED lights. *IEEE Transactions on Consumer Electronics* 50, 1 (Feb 2004), 100–107. https://doi.org/10.1109/TCE.2004.1277847

[3] Emily W Lam and Thomas DC Little. 2018. Resolving Height Uncertainty in Indoor Visible Light Positioning Using a Steerable Laser. In *2018 IEEE International Conference on Communications Workshops (ICC Workshops): The 4th Workshop on Optical Wireless Communications (OWC) (ICC 2018 Workshop - OWC)*. Kansas City, USA.

[4] S. De Lausnay, L. De Strycker, J. P. Goemaere, N. Stevens, and B. Nauwelaers. 2015. A Visible Light Positioning system using Frequency Division Multiple Access with square waves. In *2015 9th International Conference on Signal Processing and Communication Systems (ICSPCS)*. 1–7. https://doi.org/10.1109/ICSPCS.2015.7391787

[5] Tianxing Li, Qiang Liu, and Xia Zhou. 2016. Practical Human Sensing in the Light. In *Proceedings of the 14th Annual International Conference on Mobile Systems, Applications, and Services (MobiSys '16)*. ACM, New York, NY, USA, 71–84. https://doi.org/10.1145/2906388.2906401

[6] T. Little, M. Rahaim, I. Abdalla, E. Lam, R. Mcallister, and A. M. Vegni. 2018. A multi-cell lighting testbed for VLC and VLP. In *2018 Global LIFI Congress (GLC)*. 1–6. https://doi.org/10.23919/GLC.2018.8319111

[7] D. Lymberopoulos and J. Liu. 2017. The Microsoft Indoor Localization Competition: Experiences and Lessons Learned. *IEEE Signal Processing Magazine* 34, 5 (Sept 2017), 125–140. https://doi.org/10.1109/MSP.2017.2713817

[8] U. Nadeem, N. U. Hassan, M. A. Pasha, and C. Yuen. 2014. Highly accurate 3D wireless indoor positioning system using white LED lights. *Electronics Letters* 50, 11 (May 2014), 828–830. https://doi.org/10.1049/el.2014.0353

[9] U. Nadeem, N. U. Hassan, M. A. Pasha, and C. Yuen. 2015. Indoor positioning system designs using visible LED lights: performance comparison of TDM and FDM protocols. *Electronics Letters* 51, 1 (2015), 72–74. https://doi.org/10.1049/el.2014.1668

[10] H. Steendam. 2018. A 3-D Positioning Algorithm for AOA-Based VLP With an Aperture-Based Receiver. *IEEE Journal on Selected Areas in Communications* 36, 1 (Jan 2018), 23–33. https://doi.org/10.1109/JSAC.2017.2774478

[11] Jayakorn Vongkulbhisal, Bhume Chantaramolee, Yan Zhao, and Waleed S. Mohammed. 2012. A fingerprintingâĂŘbased indoor localization system using intensity modulation of light emitting diodes. *Microwave and Optical Technology Letters* 54, 5 (2012), 1218–1227. https://doi.org/10.1002/mop.26763 arXiv:https://onlinelibrary.wiley.com/doi/pdf/10.1002/mop.26763

[12] S. H. Yang, H. S. Kim, Y. H. Son, and S. K. Han. 2014. Three-Dimensional Visible Light Indoor Localization Using AOA and RSS With Multiple Optical Receivers. *Journal of Lightwave Technology* 32, 14 (July 2014), 2480–2485. https://doi.org/10.1109/JLT.2014.2327623

[13] R. Zhang, W. D. Zhong, K. Qian, and D. Wu. 2017. Image Sensor Based Visible Light Positioning System With Improved Positioning Algorithm. *IEEE Access* 5 (2017), 6087–6094. https://doi.org/10.1109/ACCESS.2017.2693299

[14] Weizhi Zhang, M. I. Sakib Chowdhury, and Mohsen Kavehrad. 2014. Asynchronous indoor positioning system based on visible light communications. *Optical Engineering* 53 (2014), 53 – 53 – 10. https://doi.org/10.1117/1.OE.53.4.045105

[15] J. Zhao, P. Ishwar, and J. Konrad. 2017. Privacy-preserving indoor localization via light transport analysis. In *2017 IEEE International Conference on Acoustics, Speech and Signal Processing (ICASSP)*. 3331–3335. https://doi.org/10.1109/ICASSP.2017.7952773